Monte Carlo simulation of cell membrane permeabilization by cold plasma

A. Zerrouki[1, 2], M. Yousfi[1], A. Rhallabi[3], H. Motomura[2], M. Jinno[2]

[1] *LAPLACE, CNRS, University of Toulouse, 118 Route de Narbonne, Toulouse, France,*
yousfi@laplace.univ-tlse.fr
[2]*Ehime University, Department of Electrical and Electronic Engineering, Matsuyama, Ehime 79-8577, Japan*
[3] *IMN, University of Nantes, 2 Rue de la Houssinière, Nantes, France.*

The aim is to simulate the pore formation of a few nanometres of width on cell multi-layer membranes during their interactions with air plasma active species (electrons, ions and radicals). This is done by developing a specific Monte Carlo model where plasma species are assumed as super-particles grouping a large number of particles (electron, ion or radical). Membrane layers were assumed to be constituted by a succession of super-sites subjected to macro-processes (recombination, reflection, activation of site, opening, etc) during the impacts by the plasma super-particles. The obtained results are very promising for a better understanding of the plasma gene transfection.

1. Introduction

Gene transfection is used to deliberately introduce DNA through membrane cells in order to confer to cells specific characteristics. It can be achieved following three different ways: chemical method, physical method and viral method [1]. All these reliable methods are limited to a few experimental systems and can have known drawbacks. Therefore, the development of a new safe and damage-free technique of gene transfection is an interesting complementary technique to the existing ones.

Gene transfection based on low temperature atmospheric pressure plasmas [2] can lead to a transient permeabilization of the cell membrane allowing processes of gene transfection in which DNA and cells are both exposed to fluxes of active plasma species (electrons, ions and neutral radicals) and also to plasma-induced electric field. However, as already stated in the literature [3], the mechanisms of more particularly membrane poration are far to be clear and controlled. Therefore fundamental understanding on plasma-induced membrane permeabilization is required for further progress in the field of plasma gene transfection.

In order to contribute to a better understanding of the pore formation through cell membranes by interactions of some plasma species with multilayer membranes, we developed a Monte Carlo poration model. The latter has been inspired from works on plasma deep silicon etching applied to nano-electronic devices (see e.g. [4]). Next section (section 2) is devoted to the description of the Monte Carlo method for simulation of pore formation while input data on reaction processes and preliminary results are discussed in section 3.

2. Monte Carlo method of membrane poration

The present model aimed to statistically simulate the pore formation during plasma interactions with membrane. The displacement of the active plasma species through the membrane and the interactions processes taken into account are governed by stochastic formalism and random numbers. Before describing Monte Carlo algorithm, it is useful to give information on the method of estimation of particle fluxes impacting the membrane, the reaction processes between plasma species and cells and the membrane structure with the corresponding discretisation domain.

2.1 Estimation of fluxes of plasma species

The proportion of the plasma species (electrons or ions or radicals) arriving to the membrane are estimated from their fluxes calculated with the help of reaction kinetics model. This model already used in the case of corona discharges in flue gases [5] is adapted to the case of air capillary plasma that has been used for gene transfection (see ref 1). The main reactions involved in this capillary discharge in ambient air have been considered in the reaction kinetics model. These reactions in phase gases before the plasma impacts with the cells are:

- Electron interactions with ambient air including N_2, O_2 and H_2O and leading to gas dissociation, excitation, ionization, attachment and also recombination between electron and positive ions
- Interactions of ions and gas leading to charge transfer, ion conversion, electron detachment and recombination between negative and positive ions

- Interactions involving excited species and leading for instance to Penning ionization
- Reaction between dissociated neutral species as radical and gas molecules

From the knowledge of reaction coefficients of these interactions between plasma and ambient air and from the knowledge of the profile of electron energy that initiate and start all these various interactions, the fluxes of electrons, ions and radicals arriving to the cell of membrane are estimated and given in section 3 (Table 1). The electron flux is the dominant one while ion flux is 100 times lower and radical flux is 1000 times lower.

2.2. Reaction processes with cell membrane

Each species is considered as a macro-species (or super-particles) representing a large number of particles.

The membrane is supposed like a multi-layer structure and each layer is supposed like a homogeneous medium of (macromolecules) of lipids or proteins. The successive interactions with membrane layers is assumed as global or macro-processes involving the incident plasma super-particles (electrons, ions and radicals) arriving to the membrane surface. The assumed macro-processes during the interactions of plasma particles with membrane layers are:

(1) Virgin layer mesh opening,
(2) Layer mesh activation leading to activated site
(3) Layer mesh opening of activated site,
(4)Particle recombination or neutralization with layer mesh
(5) Particle reflection on the internal walls of the pore.

The probabilities of occurrence of these different processes depends on the considered particle (electrons or ions or radicals) and also on the layer nature (lipid for layers 2 and 3 or protein for layers 1 and 4).

In the case of a reflection process, the particle is generally subjected to new displacements until to reach a no-void (or full) site inside the membrane layer. Finally, a specific probability of occurrence of each macro process is assigned to each super-particle based on a parametric study of the whole considered processes between plasma species and membrane. It is noteworthy that in addition to the previously obtained results [6], the different reaction probabilities have been revisited and improved for a better coherence with the bio-physical composition (lipids or proteins) of each layer of the membrane. This improvement consists to establish a relation between for instance the magnitude of the opening probability of activated site and the density magnitude of the layer (lipid or protein) on which is the activated site is opened when impacting the considered plasma species. For this example, the opening probability magnitude is inversely proportional to the layer density.

2.3. Membrane structure and discretization domain

Fig. 1 displays the *2D* simulation domain which is a superposition of 4 layers (two external protein layers with thicknesses *LY1* and *LY4* and two internal lipid layers with thicknesses *LY2* and *LY3*). The sum of the 4 layer thicknesses is chosen coherent with usual membrane thickness (for instance $LY1+LY2+LY3+LY4\approx10nm$). The simulation domain is discretised into small meshes called super-sites with step sizes *dx* and *dy* along *x* and *y* axis. Each mesh represents a large number of macro-molecules proportional to the density of the real number of molecules of lipids or proteins of the considered layer.

At the beginning of the simulation, a given plasma particle interacts first with the surface of layer 1. This is why the surface of layer 1 is initialized by an initial distribution of activated sites that are the starting point of the pore formation. The mechanisms of the formation of such initial activated sites are note described in this study. These initial activated sites when impacted by incident plasma species can be transformed into void site thus starting membrane opening.

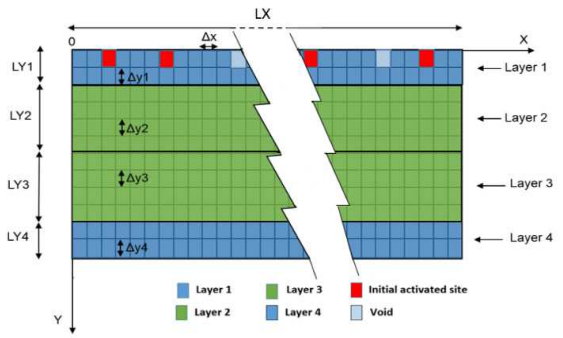

Fig.1: Multilayer membrane and discretisation domain.

2.4. Monte Carlo algorithm

A simplified flowchart of the developed Monte Carlo poration method is already given in ref [6]. It describes the successive simulation steps from the interactions with the surface of layer 1 up to the pore formation crossing the 4 considered layers following the different reaction processes described in section 2.2.

For each super-particle (electrons or ions or radicals), a specific number of initial particles is chosen proportional to the corresponding particle flux. The type of the particle *p*, its position $(x_{p,s}, y_{p,s})$ along *x* axis inside the super-site *s* and the angular distribution of the incident angle $\theta_{p,s}$ are determined from random numbers following relations given in ref 6.

The plasma parameters are chosen close to the low temperature capillary plasma generated at atmospheric pressure and used for the experimental study of gene transfection at Ehime University [1, 7]. The interactions between super-particles and super-sites are treated using predefined reaction probabilities for the different macro-processes. Before and after each process occurring in a super-site, the entire super-particle neighbours need to be identified. The Monte Carlo simulation is stopped when the entire considered numbers of each kind of super-particle is treated.

During simulation, each selected super-particle undergoes an elementary displacement *DL* until the interaction with the first super-site or a no-void (or full) site corresponding to the walls or the bottom of a given pore [6].

3. Simulation conditions, results and discussions

The simulation parameters are summarized in table 1. In this contribution, the electron energy distribution is taken into account in the improved Monte Carlo algorithm in comparison to the one previously published (ref 6).

The electron energy distribution, we assumed three different electron energy regions (25% of weak energy, 25% of average energy and 50% of high electron energy distribution). The following notations have been used for the reaction probabilities between plasma particles and membrane.

In the case of electrons interactions: Probabilities $P_{e\_weak\_Act}$, $P_{e\_avrg\_Act}$ and $P_{e\_high\_Act}$ correspond to site activation (index weak, avrg and high for weak, average and high electron distribution respectively) ; probabilities $P_{e\_weak\_Rec}$, $P_{e\_avrg\_Rec}$ and $P_{e\_high\_Rec}$ to particle recombination or neutralization inside layer mesh; probabilities $P_{e\_weak\_Op\text{-}V\text{-}s}$,$P_{e\_avrg\_Op\text{-}V\text{-}s}$; probabilities $P_{e\_high\_Op\text{-}V\text{-}s}$ to direct opening of virgin site ; and probabilities $P_{e\_weak\_Op\text{-}Act\text{-}s}$ and $P_{e\_arg\_Op\text{-}Act\text{-}s}$ and $P_{e\_high\_Op\text{-}Act\text{-}s}$ opening of activated site. As electron energy is relatively high, the electron probability reflection P_{eRefl} is assumed negligible for the present simulations.

In the case of radical/super-site and ion/super-site interactions, the predefined reaction probabilities are chosen for these preliminary calculations similar to those given in ref [6]. The reaction probabilities are P_{radOp} and P_{ionOp} (index rad for radicals and ion for ions) for opening of virgin site, $P_{radOp\text{-}Act}$ and $P_{ionOp\text{-}Act}$ for opening of activated site, P_{radRec} and P_{ionRec} for particle recombination or neutralization inside layer mesh and $P_{radRefl}$ and $P_{ionRefl}$ for particle reflection on the internal walls of the current pore. For the deviation angle distribution, the reflection processes are assumed specular.

Table.1. Parameters used for simulation

Particle number and Plasma fluxes	Total number of initial particles N_p	$1.2\text{x}10^6$ up to$1.5\text{x}10^6$ (electrons, ions and radicals)	
	Radical flux/Electron flux	10^{-3}	
	Ion flux/Electron flux	10^{-2}	
Sizes of membrane layers	Length *LX*	100	[nm]
	Membrane thickness *LY*	10	[nm]
	Layer 1 thickness *LY1*	2	[nm]
	Layer 2 thickness *LY2*	3	[nm]
	Layer 3 thickness *LY3*	3	[nm]
	Layer 3 thickness *LY4*	2	[nm]
Discretization	Step size $\Delta x=\Delta y$	0.25	[nm]
	Mesh number	16000	
	Fraction of activated sites on layer1 surface		10^{-2}

It is noteworthy that only electrons are assumed playing a role on the site activation due to their high energy in comparison ion and radical energy which are low in the considered capillary plasma in ambient air. In fact, a given super-site once activated by an electron impact is ready to be opened by an impact of either another electron or also by ion or radical.

Fig. 2a, b displays an example of pore formation without (Fig.2a) and with (Fig.2b) the effect of reflection of the ions and radicals. These two figures clearly emphasize the role of the reflection to widen the pore diameter. Then fig. 2c shows the role of the choice of the initial particle number *Np*. When the particle number is increased the obtained pores become wider and a little bite deeper when compared to Fig 2b.

In fact, the particle number can be directly correlated with the exposure time of the cell membrane to the plasma. Indeed, it is experimentally observed [1] that when cells are exposed to capillary plasma during a too short time there is no gene transfection, while when the exposure time is chosen too long, the number of survival cells decrease drastically. This what we exactly observed from Monte Carlo simulation when *Np* is chosen quite low this leads to a pore diameter

not large enough and when *Np* is chosen too high the membrane can be damaged (see Fig 2d) which normally corresponds to cell death because the most part of the membrane is damaged.

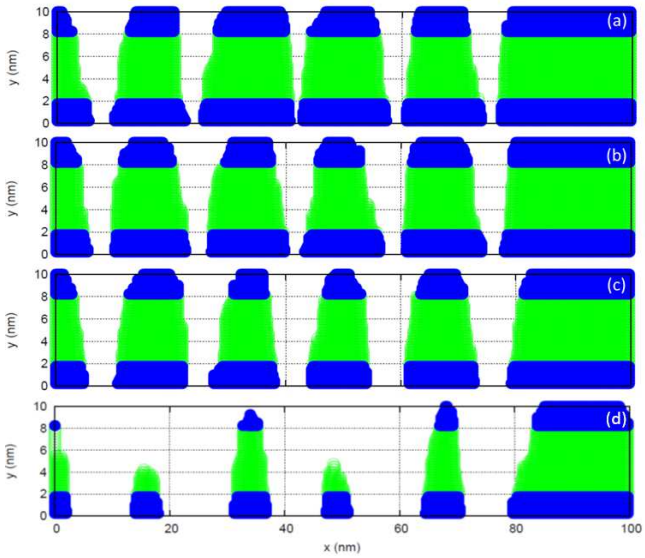

Fig. 2: Pore formation through multilayer membrane:

- **(a)** N_p*=1.2x10*^{6}, $P_{e\_weak\_Op\text{-}V\text{-}s}$ *=0,* $P_{e\_weak\_Rec}$ *=0.2 on layer 1 and 4 and 0.403 elsewhere,* $P_{e\_weak\_Act}$ *=0.795 on layer 1 and 2 and 0.59 elsewhere,* $P_{e\_weak\_Op\text{-}Act\text{-}s}$ *=0.005 on layer 1 and 4 and 0.007 elsewhere, and* $P_{e\_avrg\_Op\text{-}V\text{-}s}$ *=0,* $P_{e\_avrg\_Rec}$ *=0.15 on layer 1 and 4 and 0.304 elsewhere,* $P_{e\_avrg\_Act}$ *=0.8445 on layer 1 and 4 and 0.689 elsewhere,* $P_{e\_avrg\_Op\text{-}Act\text{-}s}$ *=0.0055 on layer 1 and 0.0077 elsewhere, and* $P_{e\_high\_Op\text{-}V\text{-}s}$ *=0,* $P_{e\_high\_Rec}$ *=0,* $P_{e\_high\_Act}$ *=0.99 on layer 1 and 0.95 on layer 2 and 3 and 0.965on layer 4,* $P_{e\_high\_Op\text{-}Act\text{-}s}$ *=0.01 on layer 1 and 0.05 on layer 2 and 3 and 0.035 on layer 4, and* $P_{radOp\text{-}V\text{-}s}$ *=* $P_{ionOp\text{-}V\text{-}s}$ *=0,* $P_{radOp\text{-}Act\text{-}s}$ *=* $P_{ionOp\text{-}Act\text{-}s}$ *=0.1 on layer 1 and 4 and 0.14 elsewhere,* P_{radRec} *=* P_{ionRec} *=1 and* $P_{radRefl}$ *=* $P_{ionRefl}$ *=0*
- **(b)** N_p*=1.2x16*^{6}*,*''same probabilities as those of fig.2a'' except for $P_{radRefl}$ *=* $P_{ionRefl}$ *=0.4 on layer 1and 4 and 0.16 elsewhere.*
- **(c)** N_p*=1.5x16*^{6}*,*''same probabilities as those of fig.2b.
- **(d)** N_p*=2x16*^{6}*,*''same probabilities as those of fig.2b.

Whereas under the chosen simulation parameters in the case of Fig 2c, the pore wideness (or diameter) is close to 10 nm which is coherent with standard diameters generally expected for gene transfection (see e.g. [8]).

Present research works are continuing for further improvements of the Monte Carlo algorithm and also for validation of the results using more particularly comparisons with AFM microscopy.

4. References

[1] M. Jinno, Y. Ikeda,H. Motomura and S. Satoh, Journal of Photopolymer Science and Technology **27** 399-404 (2014).

[2] S. Miyoshi, A.Ohkubo, N. Morikawa, Y. Ogawa, S. Nishimura, M. Fukagawa, H. Arakawa, J. Zenkyo, S. Satoh, *Patent WO/2002/064767* (2002).

[3] Y. Ogawa, N. Morikawa, A. Ohkubo-Suzuki, S. Miyoshi, H. Awakawa, Y. Kita, Biotechnol. BioEng. **92** 865 (2005).

[4] G. Marcos, A. Rhallabi and P. Ranson J. Vac. Sci. Technol. **A 21** 87 (2003)

[5] O. Eichwald, M. Yousfi et al, J. Appl. Phys., **82**, 4781-4794(1997)

[6] A. Zerrouki, M. Yousfi et al, ISPC Antwerp, Belgium (2) (2015)

[7] A. Zerrouki, Y. Sone, D. Aibara, H. Motomura, M. Jinno, ICPM5 Nara, Japan. (2014).

[8] Y. Sakai, V. Khajoee, Y. Ogawa, K. Kusuhara, Y. Katayama, T. Hara, J. of Biotech. **121** 299–308 (2006)